J Mol Model (2011) 17:21–26
DOI 10.1007/s00894-010-0700-1

ORIGINAL PAPER

A computational study of the mechanism of the unimolecular elimination of α,β-unsaturated aldehydes in the gas phase

Valentina Erastova · Jesús Rodríguez-Otero · Enrique M. Cabaleiro-Lago · Ángeles Peña-Gallego

Received: 18 December 2009 / Accepted: 1 March 2010 / Published online: 29 March 2010

Abstract The mechanism for the decarbonylation of (*E*)-2-butenal and (*E*)-2-methyl-3-pheny-2-propenal was studied with different levels of ab initio and DFT methods. Reactants, products and transition structures were optimized for two kinds of reaction channel: a one-step reaction which involves a three-membered cyclic transition state, and a two-step reaction which involves an initial four-membered cyclic transition state. According to our calculations, these two possible mechanisms entail similar energetic costs, and there are only small differences depending on the reactant. The elimination of (*E*)-2-methyl-3-pheny-2-propenal yields different products depending on the channel followed. Only one of the three possible one-step mechanisms leads directly to (*E*)-β-methylstyrene (the main product according to experiment). This fact is reasonably well reproduced by our results, since the corresponding transition state gave rise to the lowest activation Gibbs free energy.

Keywords DFT · Ab initio · Elimination · Decarbonylation · Reaction mechanism

Electronic supplementary material The online version of this article (doi:10.1007/s00894-010-0700-1) contains supplementary material, which is available to authorized users.

V. Erastova · J. Rodríguez-Otero (✉) · Á. Peña-Gallego
Departamento de Química Física, Facultade de Química,
Universidade de Santiago de Compostela,
Avda. das Ciencias s/n.,
15782 Santiago de Compostela, Spain
e-mail: r.otero@usc.es

E. M. Cabaleiro-Lago
Departamento de Química Física, Facultade de Ciencias,
Universidade de Santiago de Compostela,
Campus de Lugo, Avda. Alfonso X El Sabio s/n,
27002 Lugo, Spain

Introduction

α,β-Unsaturated aldehydes are versatile intermediates in organic synthesis. Due to the scarcity of information on the thermolysis of these compounds, Chabán et al. recently decided to carry out experimental work aimed at examining the gas-phase elimination kinetics of (*E*)-2-butenal (crotonaldehyde) and (*E*)-2-methyl-3-pheny-2-propenal (2-methylcinnamaldehyde) [1]. One of their more important objectives was to find a rational mechanism for these elimination reactions. Their favored hypothesis was that the mechanism involved a concerted process with a semi-polar three-membered cyclic transition state structure (mechanism 1 in Fig. 1). However, an alternative that Chabán et al. did not discard was a two-step reaction with a four-membered cyclic transition structure for the first stage. This implies the formation of a carbene-type intermediate and CO gas; such an intermediate may undergo 1,2-hydrogen migration to give the corresponding olefin (mechanism 2 in Fig. 1). In order to try to elucidate the mechanism for these eliminations, in this work we carry out a comprehensive computational study. The complete reaction paths for these reactions were calculated, and these results, together with the previous experimental findings, allow us to establish several interesting conclusions about the elimination reaction associated with these α,β-unsaturated aldehydes.

Computational details

All of the stationary points (reactants, products, transition structures and intermediates) of the elimination reaction of crotonaldehyde were located by optimizing every degree of freedom (except one that is maximized for the transition

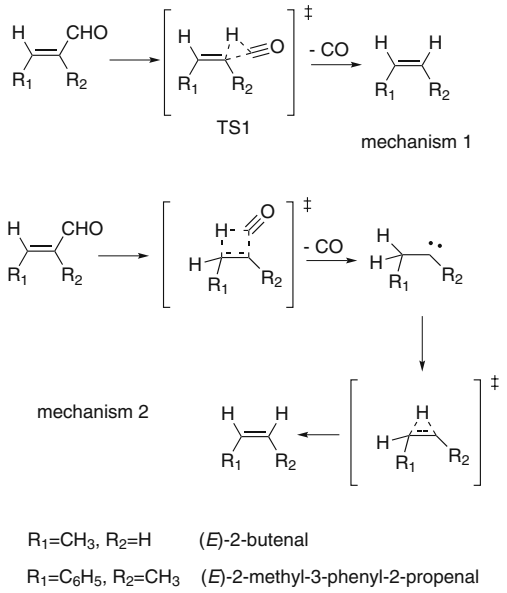

Fig. 1 The two reaction mechanisms proposed by Chabán et al. [1]

states) via ab initio methods, including electron correlation in the form of the second-order Møller–Plesset theory (MP2) and density functional theory (DFT) using the B3LYP functional. For these calculations, several basis sets with different sizes were used, ranging from 6-31G** to aug-cc-pVDZ. All of the minima and transition states were characterized from harmonic frequencies and force constants (zero negative force constants at each minimum and one negative force constant for the transition state) calculated at the same levels of theory using analytical second derivatives. This allowed us to obtain the complete profile for the Gibbs free energy at the temperature of the experimental study. The pathway for each individual reaction was obtained using the intrinsic reaction coordinate (IRC) with mass-weighted coordinates [2–4]. This allowed us to confirm the identities of all the transition states. Using the MP2-optimized geometries, single point calculations were performed at a higher correlated Møller–Plesset level (MP4SDTQ) with larger basis sets (up to aug-cc-PVTZ).

Owing to the large size of 2-methylcinnamaldehyde, and noting that quite reasonable DFT results were obtained for the elimination of crotonaldehyde, only calculations at the B3LYP/6-31+G** level were performed for the bigger compound.

Reaction enthalpies were calculated as the energy differences between products and reactants, corrected for the zero point energy and a thermal correction term for enthalpy, which was calculated from the standard expressions for an ideal gas in the canonical ensemble [5]. Activation Gibbs free energies were calculated as the energy differences between transition states and reactants, corrected for the zero point energy and a thermal correction term for Gibbs free energy.

All calculations were performed with the Gaussian 03 software package [6].

Results and discussion

Elimination of (*E*)-2-butenal (crotonaldehyde)

The *s-trans* conformation (referring to the orientation between the carbonyl double bond and the carbon–carbon double bond) of this aldehyde is more stable than the *s-cis* one, as expected. However, the energy difference is not very large: 1.3 kcal mol^{-1} at the B3LYP/6-31G* level, for example. Anyway, from here on, the *s-trans* conformation is considered the starting point of any energy scale (i.e., the reactant). The optimization of products (propene and carbon monoxide) allows us to calculate the enthalpy of reaction. Table 1 shows that B3LYP calculations lead to a slightly endothermic process. However, Møller–Plesset calculations indicate that the reactant and the products have a very similar enthalpies.

Three different structures were found (TS1a, TS1b and TS1c in Fig. 2) for the three-membered cyclic transition state of mechanism 1 (Fig. 1). All of them lead to products, but they present different characteristics. The only difference between TS1a and TS1b is the starting conformation of the reactant: *s-trans* for the former and *s-cis* for the latter. However, TS1c has a very different feature: it leads to a change in the configuration of the carbon–carbon double bond. The rotation of this double bond can be deduced from the animation of the imaginary frequency, and it can be fully confirmed via the intrinsic reaction path. Anyway, for the elimination of crotonaldehyde, the change in

Table 1 Enthalpies of reaction (kcal mol^{-1}) for the elimination of (*E*)-2-butenal calculated at various computational levels. This includes ZPE and thermal corrections to the enthalpy (T=713.75 K)

Computational level	Enthalpy of reaction (ΔH)
B3LYP/6-31G**	8.20
B3LYP/6-31+G**	7.23
B3LYP/6-31++G**	7.27
MP2/6-31G**	1.78
MP4/6-31G**//MP2/6-31G**	−1.42
MP4/6-31++G**//MP2/6-31G**	−0.92
MP2/6-31++G**	2.06
MP4/6-31++G**//MP2/6-31++G**	−0.94
MP2/aug-cc-pVDZ	2.92
MP4/aug-cc-pVDZ//MP2/aug-cc-pVDZ	−0.14
MP4/aug-cc-pVTZ//MP2/aug-cc-pVDZ	1.64

This includes ZPE and thermal corrections to the enthalpy (T=713.75 K)

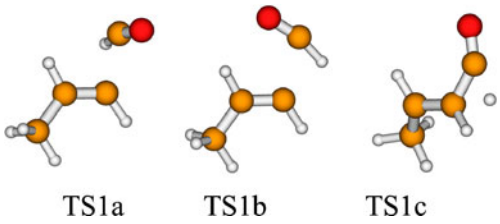

Fig. 2 The three different structures found for the three-membered cyclic transition state of mechanism 1 (Fig. 1). The MP2/aug-cc-pVDZ geometries are shown

configuration is inconsequential since the product does not change, as R_2=H. Table 2 shows that TS1a and TS1b lead to very similar activation Gibbs free energies, as expected. TS1c implies a double bond rotation and, therefore, it would be expected that a high energy cost was involved. However, it leads to a smaller activation Gibbs free energy (~4 kcal mol^{-1} in the Møller–Plesset theory). This difference is enough to state that the three-membered cyclic transition state takes place mainly through TS1c.

All attempts to find the first transition state of mechanism 2 (Fig. 1) were unsuccessful. According to our calculations (with all the levels used), simultaneous hydrogen atom migration and carbon monoxide elimination is not feasible. In all cases, searching for this structure led to a transition state where only hydrogen migration takes place. Therefore, we propose an alternative mechanism 2 (Fig. 3). Just as in the original mechanism 2, we could not find a transition state where only carbon monoxide elimination occurs, so in our alternative mechanism 2, carbon monoxide elimination takes place not in the first step but in the second step. Figure 4 shows the geometries of the transition structures and reaction intermediate for this mechanism; Table 3 includes the energetic results. A comparison between Tables 2 and 3 indicates that alternative mechanism 2 is more favorable than mechanism 1; see also Fig. 5, which summarizes the two

Table 2 Calculated activation Gibbs free energies ($\Delta G^{\ddagger}$, kcal mol^{-1}) for the three-membered cyclic transition structures involved in the elimination of (*E*)-2-butenal (Fig. 2) at *T*=713.75 K

	TS1a	TS1b	TS1c
B3LYP/6-31G**	85.17	86.77	83.65
B3LYP/6-31+G**	84.57	86.77	83.88
B3LYP/6-31++G**	84.48	86.29	83.68
MP2/6-31G**	89.62	90.68	85.56
MP4/6-31G**//MP2/6-31G**	87.62	87.93	83.70
MP4/6-31++G**//MP2/6-31G**	86.78	87.76	83.04
MP2/6-31++G**	88.40	88.31	84.85
MP4/6-31++G**//MP2/6-31++G**	86.49	85.78	83.03
MP2/aug-cc-pVDZ	83.70	85.08	79.99
MP4/aug-cc-pVDZ//MP2/aug-cc-pVDZ	82.01	82.88	78.61
MP4/aug-cc-pVTZ//MP2/aug-cc-pVDZ	82.24	82.72	78.94

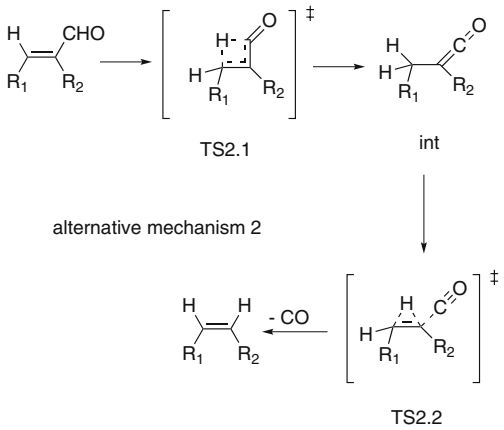

Fig. 3 An alternative mechanism for elimination through a two-step process

possible mechanisms (one-step and two-step) in an energy level diagram, including the calculated Gibbs free energies at the highest level. Therefore, according to our calculations, the elimination of (*E*)-2-butenal takes place mainly through a two-step reaction, where the second step (simultaneous hydrogen migration and carbon monoxide elimination) is the most energetically expensive process.

Another issue to be considered is the comparison between the experimental and calculated activation Gibbs free energies ($\Delta G^{\ddagger}$). There is a significant discrepancy between the experimental value (51.5 kcal mol^{-1}) and our estimation (over 70 kcal mol^{-1}). However, we think that there are several reasons to believe that the experimental value is underestimated. First, an older experimental study of this reaction predicted a substantially higher activation energy: 59.7 kcal mol^{-1} [7]. Moreover, another computational study for the one-step decarbonylation of a very similar compound (acrolein, R_1=R_2=H in Fig. 1) predicted barrier heights of 89.3 and 85.0 kcal mol^{-1} at the QCISD/cc-pVDZ and CASPT2//CASSCF(8,7)/cc-pVDZ levels, respectively [8]. Another relevant fact is that the experimental activation energy for the thermal decarbonylation of 2,2-dimethyl-3-butenal was 44.2 kcal mol^{-1} at 554.85 K [9]. Therefore, this elimination, which proceeds through a five-membered cyclic transition state, would have an activation energy that is only 7 kcal mol^{-1} lower than that for the decarbonylation of (*E*)-2-butenal. This does not

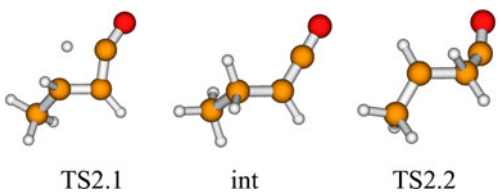

Fig. 4 Transition structures and reaction intermediate for the alternative mechanism 2 (Fig. 3). The MP2/aug-cc-pVDZ geometries are shown

Table 3 Calculated relative Gibbs free energies (kcal mol^{-1}) for the transition structures and reaction intermediate of the alternative mechanism 2 for the elimination of (*E*)-2-butenal (Figs. 3 and 4) at *T*=713.75 K

	TS2.1	int	TS2.2
B3LYP/6-31G**	67.98	3.16	77.83
B3LYP/6-31+G**	68.12	4.61	77.40
B3LYP/6-31++G**	68.07	4.57	77.31
MP2/6-31G**	72.92	2.08	79.46
MP4/6-31G**//MP2/6-31G**	71.65	2.39	77.91
MP4/6-31++G**//MP2/6-31G**	71.29	4.21	77.33
MP2/6-31++G**	72.47	4.00	78.88
MP4/6-31++G**//MP2/6-31++G**	71.09	4.23	77.40
MP2/aug-cc-pVDZ	68.76	2.28	74.87
MP4/aug-cc-pVDZ//MP2/aug-cc-pVDZ	67.27	2.41	74.10
MP4/aug-cc-pVTZ//MP2/aug-cc-pVDZ	67.09	1.37	74.34

seem reasonable considering that the five-membered cyclic transition state must have significantly less strain that the three-membered or four-membered cyclic transition state. Therefore, we think that the estimated experimental activation energy for the elimination of (*E*)-2-butenal (51.5 kcal mol^{-1}) may have been considerably underestimated.

Elimination of (*E*)-2-methyl-3-pheny-2-propenal (2-methylcinnamaldehyde)

In this case, the considerable size of this system prevents the use of high-level Møller–Plesset calculations. However, the previous study of the elimination of (*E*)-2-butenal showed that the B3LYP results were reasonably good for

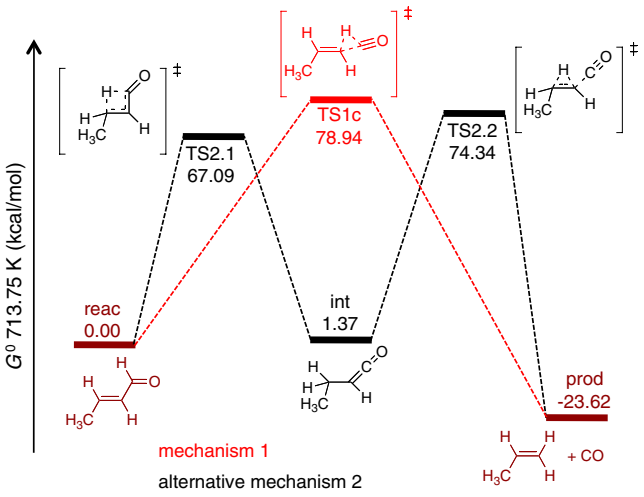

Fig. 5 Energy level diagram for the two possible mechanisms for the elimination of (*E*)-2-butenal. The calculated Gibbs free energy at the MP4/aug-cc-pVTZ//MP2/aug-cc-pVDZ level is shown (*T*=713.75 K)

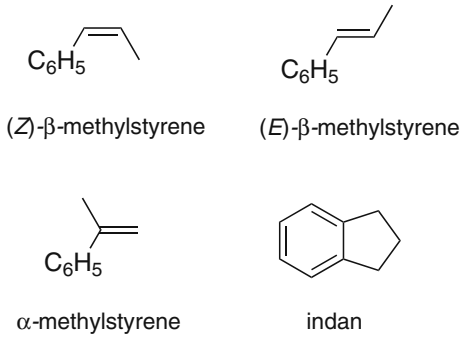

Fig. 6 Experimental products of the elimination of (*E*)-2-methyl-3-pheny-2-propenal

both geometries and energies: no substantial differences were found between the the geometries of the transition states and the reaction intermediate, and the energetic conclusions resulting from DFT and Møller–Plesset calculations were basically the same. Moreover, it was observed that the basis set has an almost negligible influence in all the B3LYP calculations. For these reasons, the elimination of (*E*)-2-methyl-3-pheny-2-propenal was only studied at the B3LYP/6-31+G** level.

The two possible products of the elimination are (*Z*)-*β*-methylstyrene and (*E*)-*β*-methylstyrene. The alternative mechanism 2 can lead to both (*Z*)-*β*-methylstyrene and (*E*)-*β*-methylstyrene, since rotation around the middle C–C single bond is possible for the reaction intermediate. However, mechanism 1 only leads to a specific product, depending on the transition structure. So, (*Z*)-*β*-methylstyrene is the product of TS1a and TS1b, whereas (*E*)-*β*-methylstyrene is the product of TS1c (owing to the change in configuration that takes place in TS1c). The experimental study showed that two other products were also obtained:

Table 4 B3LYP/6-31+G** calculated relative enthalpies and Gibbs free energies (kcal mol^{-1}) for the singular points of the elimination of (*E*)-2-methyl-3-pheny-2-propenal at *T*=743.35 K

	H	*G*
Reactant	0.00	0.00
TS1a	86.79	84.18
TS1b	90.20	85.85
TS1c	75.97	76.99[a]
TS2.1	63.26	64.83
Intermediate	9.86	8.01
TS2.2	77.32	77.77[b]
(*E*)-*β*-Methylstyrene + CO	−5.20	−32.04
(*Z*)-*β*-Methylstyrene + CO	−2.44	−28.89
α-Methylstyrene + CO	7.97	−17.75
Indan + CO	−5.19	−24.65

[a] 76.95 kcal mol^{-1} at *T*=713.75 K

[b] 77.75 kcal mol^{-1} at *T*=713.75 K

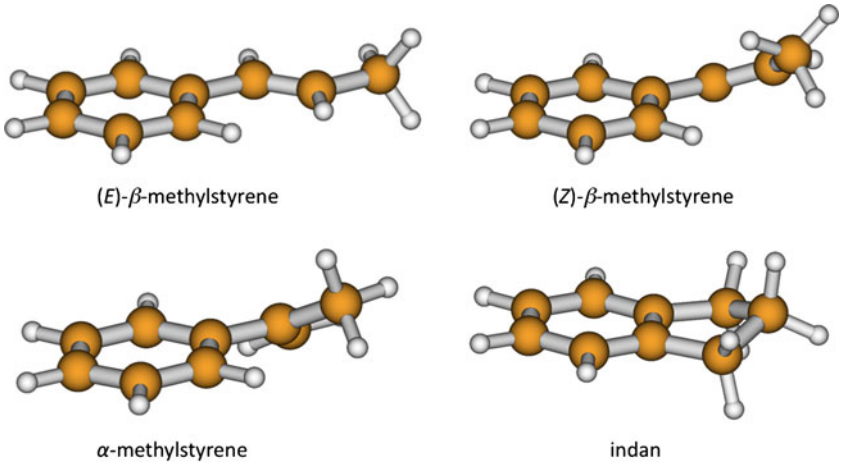

Fig. 7 Optimized geometries of the products of the elimination of (*E*)-2-methyl-3-pheny-2-propenals

α-methylstyrene and indan (Fig. 6) [1]. This fact was deduced from the very rapid isomerization of the β-methylstyrene products.

All the singular points of mechanism 1 and alternative mechanism 2 were optimized at the B3LYP/6-31+G** level. Based on the values in Table 4, the elimination of (*E*)-2-methyl-3-pheny-2-propenal takes place mainly through TS1c, and to a lesser extent through alternative mechanism 2. So, from a kinetic point of view, the formation of (*E*)-β-methylstyrene will be favored over the formation of (*Z*)-β-methylstyrene, since the main channel (TS1c) only gives rise to the (*E*) product and the secondary channel gives rise to a (*E*)/(*Z*) mixture. This agrees rather well with the experimental results, since the obtained distribution was 42.7% (*E*)-β-methylstyrene and 13.7% (*Z*)-β-methylstyrene. Chabán et al. suggested that the distribution of products is a consequence of thermodynamic considerations [1]. However, in our opinion, several facts point to a kinetic control. Firstly, the product distribution barely changes over time, and changes only slightly with temperature. Moreover, according to our results (Table 4), the difference in energy between the two isomeric products should lead to a larger difference between the amounts of each produced. Table 4 also shows that both isomers give rise to exothermic and very exergonic processes, but from the difference in reaction Gibbs energies, a ratio of 10:1 would be expected for the (*E*)/(*Z*) product distribution. Besides the two β-methylstyrene isomers, experimental work shows that two other products are produced: α-methylstyrene (29.4 %) and indan (14.4 %). Evidently, this fact cannot be explained from a thermodynamic point of view either, since α-methylstyrene is clearly the less stable product (actually, its production is the only endothermic process). In general, from the results of Table 4, it is clear that the experimental distribution of the products is not related to their energetic stabilities; this is another argument against thermodynamic control.

The most stable of the three methylstyrene products is the isomer (*E*)-β-methylstyrene. This fact is easily explained by the optimized geometry: only this isomer can adopt a fully planar disposition where the external C=C double bond gets the highest delocalization with the π cloud of the phenyl group. However, in (*Z*)-β-methylstyrene and, especially, in α-methylstyrene, steric repulsion prevents a planar disposition (Fig. 7). Indan is enthalpically as favored as (*E*)-β-methylstyrene as a product, but it is entropically penalized.

According to Table 4, α-methylstyrene is the considerably less stable product. However, a significant amount (29.4 %) of this product is found experimentally. A plausible explanation for this fact could be that α-methylstyrene derives from the isomerization of the main

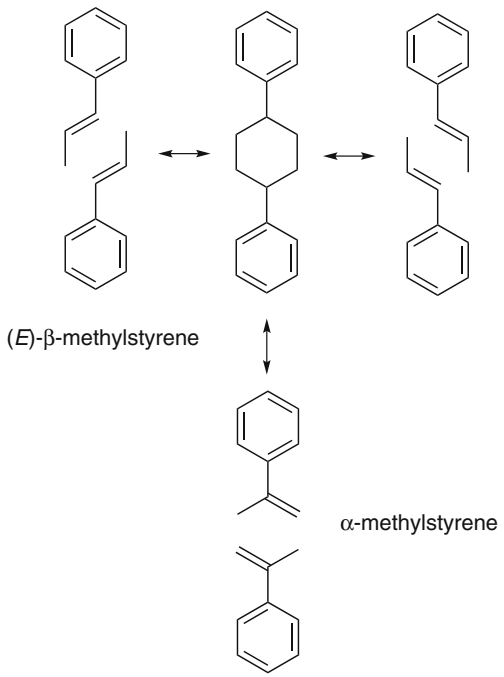

Fig. 8 A possible path for the formation of α-methylstyrene

product, (*E*)-β-methylstyrene. Recently, Lin et al. have proposed a mechanism for the dimerization of (*E*)-β-methylstyrene at a temperature of about 100 °C, in which 1,4-diphenylcyclohexane could be involved (Fig. 8) [10]. If 1,4-diphenylcyclohexane is present, then it is not difficult to postulate the mechanism for α-methylstyrene formation; thus, either (*E*)-β-methylstyrene or α-methylstyrene will be produced, depending on which C–C single bond is broken (in both cases, the reaction is basically the formation of two molecules of propene from cyclohexane).

Conclusions

In agreement with experimental work [1], our calculations have shown that the elimination of (*E*)-2-butenal and (*E*)-2-methyl-3-pheny-2-propenal takes place through a three- or a four-membered cyclic transition state, via a one-step or a two-step mechanism, respectively. For this second mechanism, we have proposed an alternative to the original second mechanism proposed (with only slight differences), because it was not possible to find the transition structure suggested for the first step in the original second mechanism. The energetic results showed that both mechanisms incur similar energy costs, but there are small differences between the elimination of (*E*)-2-butenal and (*E*)-2-methyl-3-pheny-2-propenal. However, these small differences can lead to important consequences. Therefore, the elimination of (*E*)-2-butenal takes place mainly through a two-step reaction, with the second step (simultaneous hydrogen migration and carbon monoxide elimination) being the most energetically expensive process. However, the elimination of (*E*)-2-methyl-3-pheny-2-propenal takes place mainly through the one-step mechanism (with a three-membered cyclic transition state), and to a lesser extent through the two-step mechanism. Moreover, the most favorable three-membered cyclic transition state is TS1c, in which a change in the configuration of the carbon–carbon double bond takes place. This configurational change leads to (*E*)-β-methylstyrene as the product, and this has been found to be the main product experimentally.

Acknowledgments The authors thank the Xunta de Galicia for financial support ("Axuda para a Consolidación e Estructuración de unidades de investigación competitivas do Sistema Universitario de Galicia, 2007/50, cofinanciada polo FEDER 2007-2013"). The authors also wish to express their gratitude to the CESGA (Centro de Supercomputación de Galicia).

References

1. Chabán OY, Domínguez RM, Herize A, Tosta M, Cuenca A, Chuchani G (2007) J Phys Org Chem 20:307–312
2. Fukui K (1981) Acc Chem Res 14:363–368
3. González C, Schlegel HB (1989) J Phys Chem 90:2154–2161
4. González C, Schlegel HB (1990) J Phys Chem 94:5523–5527
5. McQuarrie DA (1973) Statistical thermodynamics. Harper and Row, New York
6. Frisch MJ, Trucks GW, Schlegel HB, Scuseria GE, Robb MA, Cheeseman JR, Montgomery JA Jr, Vreven T, Kudin KN, Burant JC, Millam JM, Iyengar SS, Tomasi J, Barone V, Mennucci B, Cossi M, Scalmani G, Rega N, Petersson GA, Nakatsuji H, Hada M, Ehara M, Toyota K, Fukuda R, Hasegawa J, Ishida M, Nakajima T, Honda Y, Kitao O, Nakai H, Klene M, Li X, Knox JE, Hratchian HP, Cross JB, Bakken V, Adamo C, Jaramillo J, Gomperts R, Stratmann RE, Yazyev O, Austin AJ, Cammi R, Pomelli C, Ochterski JW, Ayala PY, Morokuma K, Voth GA, Salvador P, Dannenberg JJ, Zakrzewski VG, Dapprich S, Daniels AD, Strain MC, Farkas O, Malick DK, Rabuck AD, Raghavachari K, Foresman JB, Ortiz JV, Cui Q, Baboul AG, Clifford S, Cioslowski J, Stefanov BB, Liu G, Liashenko A, Piskorz P, Komaromi I, Martin RL, Fox DJ, Keith T, Al-Laham MA, Peng CY, Nanayakkara A, Challacombe M, Gill PMW, Johnson B, Chen W, Wong MW, Gonzalez C, Pople JA (2004) Gaussian 03, revision C.02. Gaussian, Wallingford
7. Grela MA, Colussi AJ (1986) J Phys Chem 90:434–437
8. Fang WH (1999) J Am Chem Soc 121:8376–8384
9. Crawford RJ, Lutener S, Tokunaga H (1977) Can J Chem 55:3951–3954
10. Lin SY, Tseng JM, Lin YF, Huang WT, Shu CM (2008) J Therm Anal Cal 93:257–267